A Melanocortin 1 Receptor Allele Suggests Varying Pigmentation Among Neanderthals

Carles Lalueza-Fox,[1]*† Holger Römpler,[2,10]* David Caramelli,[3] Claudia Stäubert,[2] Giulio Catalano,[3,4] David Hughes,[9] Nadin Rohland,[9] Elena Pilli,[3] Laura Longo,[5] Silvana Condemi,[6] Marco de la Rasilla,[7] Javier Fortea,[7] Antonio Rosas,[8] Mark Stoneking,[9] Torsten Schöneberg,[2] Jaume Bertranpetit,[4] Michael Hofreiter[9]†

The melanocortin 1 receptor (MC1R) regulates pigmentation in humans and other vertebrates. Variants of MC1R with reduced function are associated with pale skin color and red hair in humans of primarily European origin. We amplified and sequenced a fragment of the MC1R gene (*mc1r*) from two Neanderthal remains. Both specimens have a mutation that was not found in ~3700 modern humans analyzed. Functional analyses show that this variant reduces MC1R activity to a level that alters hair and/or skin pigmentation in humans. The impaired activity of this variant suggests that Neanderthals varied in pigmentation levels, potentially on the scale observed in modern humans. Our data suggest that inactive MC1R variants evolved independently in both modern humans and Neanderthals.

One gene responsible for skin and hair color variation in humans is *melanocortin 1 receptor* (*mc1r*), which encodes a seven-transmembrane heterotrimeric GTP-binding protein (G protein)–coupled receptor (GPCR) (Fig. 1) (*1*). Red hair and pale skin result from both complete and partial loss-of-function alleles in human MC1R (huMC1R) because they alter the balance between eumelanin and pheomelanin synthesis (*2*). Thus, we hypothesize that the retrieval of *mc1r* sequences from extinct species can potentially provide information on their phenotypic traits.

Neanderthals are an extinct hominid group that lived in Eurasia ~400,000 to 28,000 years ago (*3*). Recently, metagenomic approaches recovered about 1 megabase of the Neanderthal genome (*4*, *5*), implying that amplification of nuclear DNA by the polymerase chain reaction (PCR) may be feasible in well-preserved Neanderthal remains. We studied two Neanderthal fossils, Monti Lessini (Italy) (*6*) and El Sidrón 1252 (Spain) (*7*). Both samples have a low degree of amino acid racemization (<0.10) and high amino acid content (>20,000 parts per million), suggesting good DNA preservation (*8*). Amplifications of the hypervariable region 1 of the mitochondrial DNA showed that endogenous Neanderthal DNA was preserved in these individuals (*6*, *9*).

We assumed that retrieval of Neanderthal nuclear DNA sequences from these samples was possible if the amplicon length was short and large numbers of clones were generated. Because of the low level of divergence between Neanderthals and modern humans, it is impossible to distinguish contamination if the sequences are identical or polymorphisms are shared between the species (*10*). Therefore, we focused on identifying Neanderthal-specific substitutions. We successfully amplified a 128–base pair (bp) fragment of *mc1r* (*11*) from the Monti Lessini sample. Most clones were identical to the modern human sequence, most likely representing contamination of the Neanderthal bone with modern human DNA. However, 1 of the 25 clones had an A-to-G substitution at nucleotide position 919, resulting in an Arg-to-Gly change at amino acid position 307, which was not previously observed in modern humans (*12*, *13*). We hypothesized that this was not due to PCR error, because most errors are C-to-T (or G-to-A) changes, due to cytosine deaminations in the template DNA (*14*, *15*).

Because the number of amplifiable ancient DNA molecules increases exponentially with decreasing amplification length (*16*), we designed primers to amplify a shorter DNA fragment and performed four different amplifications for El Sidrón 1252 and one for Monti Lessini. We sequenced at least 10 clones per reaction.

[1]Departament de Biologia Animal, Universitat de Barcelona, Spain. [2]Department of Molecular Biochemistry, Medical Faculty, University of Leipzig, Leipzig, Germany. [3]Department of Animal Biology and Genetics, Laboratory of Anthropology, University of Florence, Italy. [4]Unitat de Biologia Evolutiva, Universitat Pompeu Fabra, Barcelona, Spain. [5]Dipartimento di Scienze Ambientali, Università di Siena, Siena, Italy. [6]Unité d'Anthropologie, CNRS, UMR 6578, Marseille, France. [7]Área de Prehistoria, Universidad de Oviedo, Spain. [8]Departamento de Paleobiología, Museo Nacional de Ciencias Naturales, CSIC, Madrid, Spain. [9]Department of Evolutionary Genetics, Max Planck Institute for Evolutionary Anthropology, Leipzig, Germany. [10]Department of Organismic and Evolutionary Biology, Harvard University, Cambridge, MA, USA.

*These authors contributed equally to this work.
†To whom correspondence should be addressed. E-mail: clalueza@ub.edu (C.L.-F.); hofreite@eva.mpg.de (M.H.)

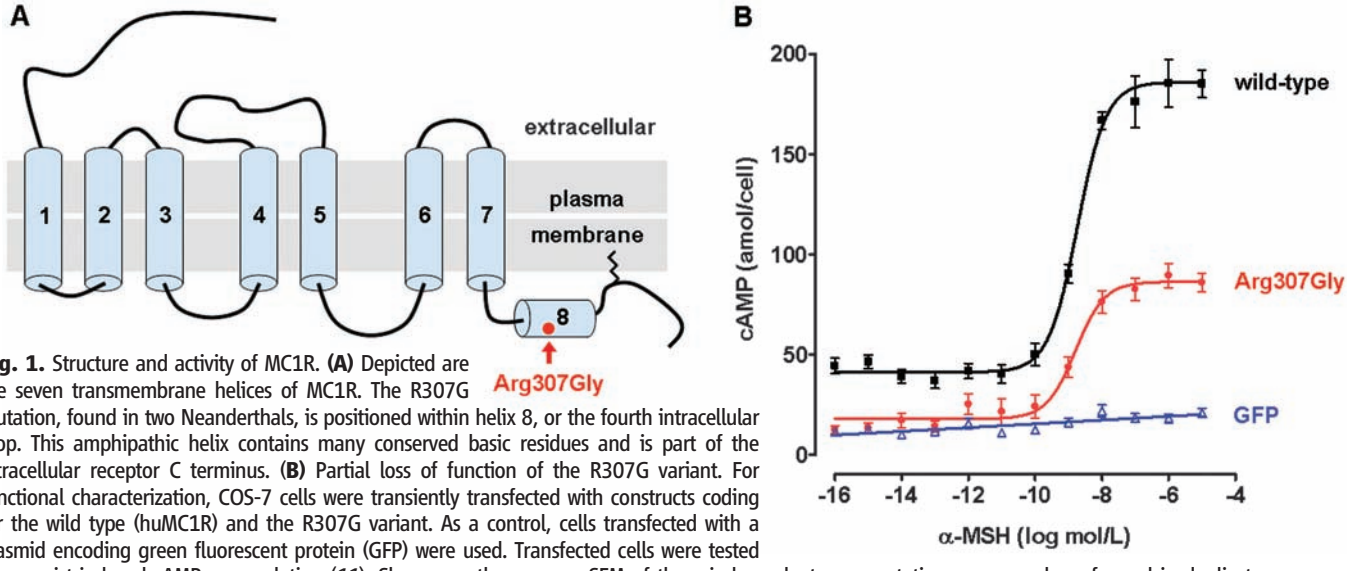

Fig. 1. Structure and activity of MC1R. **(A)** Depicted are the seven transmembrane helices of MC1R. The R307G mutation, found in two Neanderthals, is positioned within helix 8, or the fourth intracellular loop. This amphipathic helix contains many conserved basic residues and is part of the intracellular receptor C terminus. **(B)** Partial loss of function of the R307G variant. For functional characterization, COS-7 cells were transiently transfected with constructs coding for the wild type (huMC1R) and the R307G variant. As a control, cells transfected with a plasmid encoding green fluorescent protein (GFP) were used. Transfected cells were tested for agonist-induced cAMP accumulation (*11*). Shown are the mean ± SEM of three independent representative assays, each performed in duplicate.

The Arg^{307}→Gly^{307} (R307G) substitution was present in all amplification products at frequencies ranging from 7 to 25% (fig. S1). Because the humanlike sequences probably at least partially represent contamination with modern human DNA, we cannot decide whether the two individuals are homozygous for R307G or heterozygous. Thus, we concentrated on authentication of the R307G variant. The likelihood of an incorrect nucleotide, due to postmortem damage or PCR errors, decreases as the number of independent amplifications increases (*14*). Therefore, we amplified a different Monti Lessini extract in two additional laboratories with different primer sets. The R307G substitution was found in all three laboratories for the Monti Lessini sample but only in Barcelona for the El Sidrón sample. Altogether, we observed this substitution in 9 of 12 amplifications, with frequencies ranging from 4 to 36% (table S1). Moreover, there is no known damage in ancient DNA resulting in A-to-G substitutions (*15*). Even if our results were due to a previously unknown kind of template damage that occurs at the same frequency as cytosine deamination (2%) (*14*), the probability of obtaining the same result in 9 out of 12 independent amplifications is $\sim 10^{-13}$ (*11*). These results suggest that the R307G substitution is a reproducible, albeit minority, sequence not attributable to damage.

The R307G substitution has not been described in more than 2800 modern humans that have been fully sequenced for *mc1r* (*12*, *13*). We genotyped this polymorphism in the CEPH Human Genome Diversity Panel (*17*) (fig. S2), as well as in all people involved in the excavation and genetic analysis, to determine whether this variant exists in extant humans (*11*). No individual had the R307G allele. If the R307G allele occurs in modern humans, it must be at a very low frequency, and it is unlikely that such a rare variant would appear as contamination in three separate laboratories. We additionally investigated whether nonhuman contamination could explain this result. BLASTN was used to compare the longest sequence with the R307G variant and showed that it was most like human, with 98% sequence similarity, followed by primate sequences with progressively decreasing identity (table S4). None of the sequences in GenBank matched perfectly to the R307G variant, and nonprimate mammalian sequences differ considerably, excluding other common sources of contamination as possible origins of the sequence. Therefore, we concluded that the R307G substitution is an endogenous Neanderthal sequence.

The R307G mutation is positioned at the cytoplasmatic surface of MC1R within the so-called helix 8 or fourth intracellular loop (*18*, *19*) (Fig. 1A). Mutations of conserved basic residues within this amphipathic helix alter receptor function in numerous GPCRs (*19*, *20*). Although Arg^{307} is replaced by Lys in fox, cow, and sheep and by Met in mouse (*21*), the position has been shown to be intolerant of most mutations (*22*) (fig. S5). To investigate whether the R307G substitution affects the function of huMC1R, both wild-type MC1R and the R307G variant were expressed in COS-7 cells, and basal and agonist-induced intracellular cyclic adenosine monophosphate (cAMP) levels were determined. huMC1R responded to the natural agonist α–melanocyte-stimulating hormone (α-MSH) with an ~fourfold increase in intracellular cAMP levels (Fig. 1B and table S2). In contrast, cells expressing the R307G variant had intracellular cAMP levels that were 40% of the wild-type levels and were 50% less than wild-type levels when activated by an agonist. Whereas basal cAMP levels of the wild type strongly correlated with the amount of transfected plasmid DNA, this was not the case for the basal activity of R307G (fig. S3). Analysis of the stimulation curves (Fig. 1B) showed that the median effective concentration values did not differ between the human and R307G variants. To exclude the possibility that the observed differences resulted from overexpression in COS-7 cells, we established stable cell lines with a single expression cassette of either MC1R variant at a predefined locus (*11*). These stably transfected CHOK1 cells also showed reduced agonist-induced cAMP levels for the R307G variant (table S2).

In order to determine whether these reduced basal and agonist-induced cAMP levels observed in R307G were caused by either lower cell-surface expression levels (fig. S4) or reduced G-protein coupling properties, we determined MC1R protein expression levels with an enzyme-linked immunosorbent assay and performed binding assays on intact cells (*11*). Total expression of the full-length receptor protein did not differ between the two variants (table S3). In contrast, radioligand binding and ligand-binding–independent measurements revealed substantially reduced cell-surface expression of the R307G variant (table S3). However, we observed no difference in the ability of both receptor variants to bind α-MSH (table S3). Altogether, our data support the idea that the R307G allele has a partial loss of function caused by reduced cell-surface expression of receptor protein (*23*, *24*) and altered G protein–coupling efficacy.

Alleles conferring partial loss of function of MC1R have been associated with pale skin color and red hair in humans (*1*, *12*). We tested a functional cAMP assay on extant partially functional huMC1R alleles associated with pale skin color and red hair. We confirmed partial activity of these variants, indistinguishable from that of R307G (table S2). Pale skin color and lighter hair are more likely when MC1R alleles are in a homozygote or compound heterozygote stage. Although we cannot decide currently whether the Neanderthal individuals analyzed were homozygous for R307G or heterozygous, we can obtain a minimum frequency for this variant in Neanderthals. If we assume that both individuals were heterozygous, we obtain a minimum allele frequency for R307G of 50% for the two individuals investigated. From this figure, the minimum frequency of the mutation in all Neanderthals that is compatible with observing two mutant alleles when four alleles are sampled at random is 0.1 for $P > 0.05$. This translates into at least 1% of homozygous Neanderthal individuals that may have had reduced pigmentation levels, possibly even similar to the pale skin color and/or red hair observed in modern humans. These results once more raise the question of whether reduced pigmentation may have been advantageous in Europe, for example via ultraviolet-light–mediated vitamin D synthesis, or whether it just reflects a loss of constraint for the *mc1r* gene in regions of reduced solar irradiation (*25*). Our data do not support the hypothesis that phenotypic similarities between these two human groups are explained by gene flow (*26*) and do support the hypothesis of convergent evolution of reduced-function MC1R alleles, as suggested between modern European and Asian populations (*27*, *28*).

References and Notes

1. J. L. Rees, *Annu. Rev. Genet.* **37**, 67 (2003).
2. J. L. Rees, *Pigment Cell Res.* **13**, 135 (2000).
3. C. Finlayson *et al.*, *Nature* **443**, 850 (2006).
4. R. E. Green *et al.*, *Nature* **444**, 330 (2006).
5. J. P. Noonan *et al.*, *Science* **314**, 1113 (2006).
6. D. Caramelli *et al.*, *Curr. Biol.* **16**, R630 (2006).
7. A. Rosas *et al.*, *Proc. Natl. Acad. Sci. U.S.A.* **103**, 19266 (2006).
8. D. Serre *et al.*, *PLoS Biol.* **2**, e57 (2004).
9. C. Lalueza-Fox *et al.*, *Curr. Biol.* **16**, R629 (2006).
10. S. Pääbo, *Trends Biochem. Sci.* **24**, M13 (1999).
11. Materials and methods are available as supporting material on *Science* Online.
12. T. H. Wong, J. L. Rees, *Peptides* **26**, 1965 (2005).
13. M. R. Gerstenblith, A. M. Goldstein, M. C. Fargnoli, K. Peris, M. T. Landi, *Hum. Mutat.* **28**, 495 (2007).
14. M. Hofreiter, V. Jaenicke, D. Serre, A. v. Haeseler, S. Pääbo, *Nucleic Acids Res.* **29**, 4793 (2001).
15. M. Stiller *et al.*, *Proc. Natl. Acad. Sci. U.S.A.* **103**, 13578 (2006).
16. H. N. Poinar *et al.*, *Science* **311**, 392 (2006).
17. H. M. Cann *et al.*, *Science* **296**, 261b (2002).
18. T. Okuno, T. Yokomizo, T. Hori, M. Miyano, T. Shimizu, *J. Biol. Chem.* **280**, 32049 (2005).
19. N. M. D. Santos, L. A. Gardner, S. W. White, S. W. Bahouth, *J. Biol. Chem.* **281**, 12896 (2006).
20. M. Tetsuka, Y. Saito, K. Imai, H. Doi, K. Maruyama, *Endocrinology* **145**, 3712 (2004).
21. B. K. Rana *et al.*, *Genetics* **151**, 1547 (1999).
22. P. A. Kanetsky *et al.*, *Cancer Epidemiol. Biomarkers Prev.* **13**, 808 (2004).
23. K. A. Beaumont *et al.*, *Hum. Mol. Genet.* **14**, 2145 (2005).
24. B. L. Sanchez-Laorden, J. Sanchez-Mas, M. C. Turpin, J. C. Garcia-Borron, C. Jimenez-Cervantes, *Cell Mol. Biol.* **52**, 39 (2006).
25. R. M. Harding *et al.*, *Am. J. Hum. Genet.* **66**, 1351 (2000).
26. M. H. Wolpoff, J. H. R. Caspari, *Am. J. Phys. Anthropol.* **112**, 129 (2000).
27. S. Myles, M. Somel, K. Tang, J. Kelso, M. Stoneking, *Hum. Genet.* **120**, 613 (2007).
28. H. L. Norton *et al.*, *Mol. Biol. Evol.* **24**, 710 (2007).

29. We thank C. Green for many suggestions and critical reading of the manuscript; S. Ptak for help with the statistical analysis; and the Ministry of Education and Science of Spain and the Generalitat de Catalunya (C.L.F. and J.B.), the Max Planck Society (D.H., N.R., M.S., and M.H.), the Deutsche Forschungsgemeinschaft, Bundesministerium für

Bildung und Forschung, the IZKF Leipzig (H.R., C.S., and T.S.), and the Studienstiftung des Deutschen Volkes (C.S.) for financial support. The excavation at El Sidrón is supported by the Autonomous Government of Asturias. The study of the Monti Lessini Neanderthal is framed into a research project on human fossil remains at the Verona Natural History Museum. The Neanderthal *mc1r* sequence has been deposited at GenBank, accession number EU204643.

Supporting Online Material
www.sciencemag.org/cgi/content/full/1147417/DC1
Materials and Methods
Figs. S1 to S5
Tables S1 to S4
References

5 July 2007; accepted 12 October 2007
Published online 25 October 2007;
10.1126/science.1147417
Include this information when citing this paper.

5′-Triphosphate–Dependent Activation of PKR by RNAs with Short Stem-Loops

Subba Rao Nallagatla,[1]* Jungwook Hwang,[2]* Rebecca Toroney,[1] Xiaofeng Zheng,[1,3] Craig E. Cameron,[2,4]† Philip C. Bevilacqua[1]†

Molecular patterns in pathogenic RNAs can be recognized by the innate immune system, and a component of this response is the interferon-induced enzyme RNA-activated protein kinase (PKR). The major activators of PKR have been proposed to be long double-stranded RNAs. We report that RNAs with very limited secondary structures activate PKR in a 5′-triphosphate–dependent fashion in vitro and in vivo. Activation of PKR by 5′-triphosphate RNA is independent of RIG-I and is enhanced by treatment with type 1 interferon (IFN-α). Surveillance of molecular features at the 5′ end of transcripts by PKR presents a means of allowing pathogenic RNA to be distinguished from self-RNA. The evidence presented here suggests that this form of RNA-based discrimination may be a critical step in mounting an early immune response.

The innate immune response offers the host early protection from foreign organisms and viruses (*1*). As part of this response, the double-stranded RNA (dsRNA)–activated protein kinase (PKR) becomes activated through autophosphorylation in the presence of viral RNA (*2*). Subsequently, PKR phosphorylates eukaryotic initiation factor 2α (eIF2α), which inhibits translation initiation, thus preventing pathogen replication (*2*).

PKR can be both activated and inhibited through its interaction with RNA, which is mediated by dsRNA-binding motifs (dsRBMs) (Fig. 1A) that also exist in other diverse proteins, including RNA-specific adenosine deaminases (ADARs), Dicer, and ribonuclease III (*3*). This interaction with dsRNA is sequence-independent (*4*, *5*), and although at least 16 base pairs (bp) of dsRNA are required for inhibition of PKR, 33 bp are needed for activation (*4*, *6*). We have previously shown that short dsRNAs with single-stranded tails (ss-dsRNAs) activate PKR, with the length of the tail providing a critical determinant (*6*). This motif has an imperfect stem of 16 bp and is flanked by single-stranded tails (Fig. 1B), and because it was prepared by transcription, it contains a 5′-triphosphate (*7*). This raises the question of what features of the tail might be important in activating PKR.

In our initial experiments, we observed that a 79-bp perfectly dsRNA (dsRNA-79) led to potent activation of PKR, with an RNA-dependency factor of ~35 (Fig. 1C) (*8*). PKR was also activated by ss-dsRNAs and gave the expected ~10-nucleotide (nt) tail-length dependence (*6*) (Fig. 1C). Maximal activation by ss-dsRNA was as intense as that by dsRNA-79, albeit requiring ~10-fold more RNA. The ss-dsRNA(9,11) (having 5′ and 3′ tails of 9 and 11 nt, respectively) transcript (Fig. 1B) was next treated with calf intestinal phosphatase (CIP) to remove the 5′-triphosphate (fig. S1), leading to abrogation of activation even at higher concentrations (Fig. 1C). Furthermore, chemically synthesized ss-dsRNA(9,11) having a 5′ hydroxyl (fig. S2) also failed to activate PKR. The presence of the 5′-triphosphate led to 100-fold higher PKR activation than occurred in its absence (fig. S2) (*8*). A mixture of CIP-treated and untreated transcripts showed full activation of PKR (fig. S3), indicating that the reason why CIP-treated RNAs do not activate PKR is not because CIP treatment renders PKR incapable of activation.

To test whether the presence of 5′-triphosphate also affects the ability of long dsRNAs to activate PKR, top and bottom strands of dsRNA-79 were CIP-treated and annealed (fig. S4). Unlike ss-dsRNA, CIP-treated as well as untreated dsRNA could activate PKR, with a standard bell-shaped dependence on RNA concentration (fig. S4D) (*6*). Thus, long dsRNA does not require 5′-triphosphate, suggesting that the contribution of this motif to PKR activation is dependent on RNA structure.

Given that ss-dsRNAs have functionally important non–base-paired elements (*6*), we next tested activation by the single strands of dsRNA-79, which also have secondary structure (fig. S4, A and B). CIP-treated ssRNA-79TS (TS, top

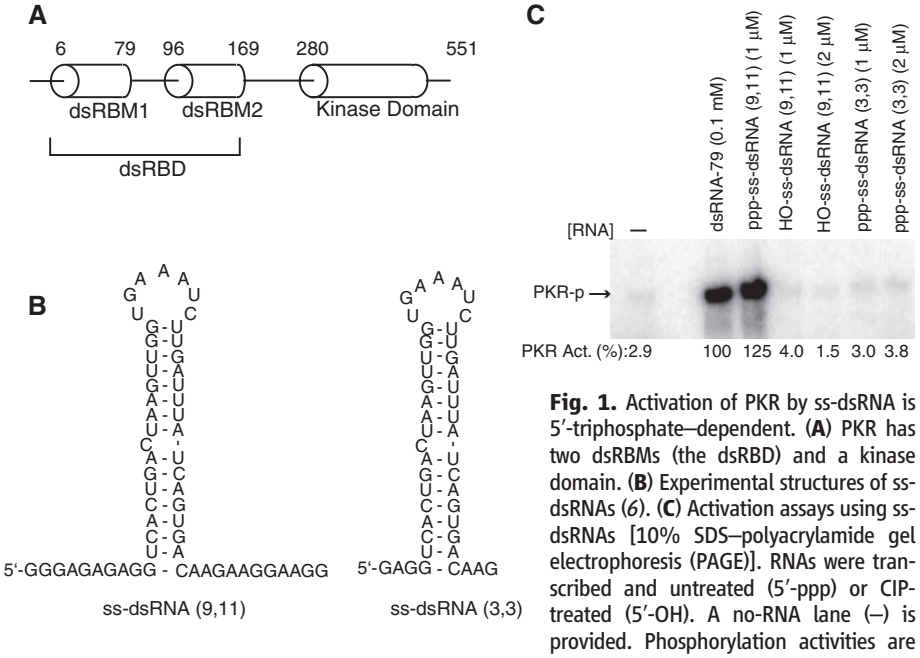

Fig. 1. Activation of PKR by ss-dsRNA is 5′-triphosphate–dependent. (**A**) PKR has two dsRBMs (the dsRBD) and a kinase domain. (**B**) Experimental structures of ss-dsRNAs (*6*). (**C**) Activation assays using ss-dsRNAs [10% SDS–polyacrylamide gel electrophoresis (PAGE)]. RNAs were transcribed and untreated (5′-ppp) or CIP-treated (5′-OH). A no-RNA lane (—) is provided. Phosphorylation activities are normalized to 0.1 μM dsRNA-79 (no CIP).

[1]Department of Chemistry, Pennsylvania State University, University Park, PA 16802, USA. [2]Integrative Biosciences, Pennsylvania State University, University Park, PA 16802, USA. [3]Department of Biochemistry and Molecular Biology, Life Sciences College, Peking University, Beijing 100871, China. [4]Department of Biochemistry and Molecular Biology, Pennsylvania State University, University Park, PA 16802, USA.

*These authors contributed equally to this work.
†To whom correspondence should be addressed. E-mail: pcb@chem.psu.edu (P.C.B.); cec9@psu.edu (C.E.C.)